· Article · Advances in Polar Science
doi: 10.13679/j.advps.2022.0017 December 2022 Vol. 33 No. 4: 313-325

Spatial distribution of aloricate ciliates in the stratified water of the Cosmonaut and Cooperation Seas in the Southern Ocean

LI Jingyuan[1,2,3,4], LI Haibo[1,2,3*], WANG Chaofeng[1,2,3], ZHANG Wuchang[1,2,3*] & XIAO Tian[1,2,3]

[1] CAS Key Laboratory of Marine Ecology and Environmental Sciences, Institute of Oceanology, Chinese Academy of Sciences, Qingdao 266071, China;
[2] Laboratory for Marine Ecology and Environmental Science, Qingdao National Laboratory for Marine Science and Technology, Qingdao 266237, China;
[3] Center for Ocean Mega-Science, Chinese Academy of Sciences, Qingdao 266071, China;
[4] University of Chinese Academy of Sciences, Beijing 100049, China

Received 22 August 2022; accepted 28 December 2022; published online 30 December 2022

Abstract Aloricate ciliates are the main component of microzooplankton. They play important roles in the circulation of materials and flow of energy in marine pelagic ecosystems. To determine the distribution pattern and structure of the aloricate ciliate community in vertically stratified waters of the Southern Ocean, we collected data on aloricate ciliates in the Cosmonaut and Cooperation Seas during the 36th Chinese National Antarctic Research Expedition. The ranges of aloricate ciliate abundance and biomass were 5–3097 ind·L^{-1} and 0.01–11.40 μg C·L^{-1}, respectively. Vertically, the average abundance of aloricate ciliates decreased from the surface to 200 m, while biomass was highest in the 50-m layer. The importance of aloricate ciliates <20 μm increased along the depth gradient. Their contribution to total abundance increased from 13.04% in the surface layer to 73.71% in the 200-m layer. This is the first study to explore the distribution characteristics of the aloricate ciliate community in a stratified water column of the Southern Ocean. Our results will be helpful for understanding the variation in the pelagic community in waters of the Southern Ocean with intensified stratification.

Keywords **aloricate ciliates, spatial distribution, community structure, stratification, Southern Ocean**

Citation: Li J Y, Li H B, Wang C F, et al. Spatial distribution of aloricate ciliates in the stratified water of the Cosmonaut and Cooperation Seas in the Southern Ocean. Adv Polar Sci, 2022, 33(4): 313-325, doi: 10.13679/j.advps.2022.0017

1 Introduction

Planktonic ciliates, which have a size range of 10–200 μm, are ubiquitous in all kinds of marine environments (Li et al., 2016, 2020, 2022; Yang et al., 2016; Monti-Birkenmeier et al., 2017; Liang et al., 2018). They are composed of aloricate ciliates and tintinnids, belonging to the subclasses Oligotrichia and Choreotrichia, respectively. Aloricate ciliates, the major component of planktonic ciliates, usually dominate the planktonic ciliate community and microzooplankton community in coastal waters (Zhang et al., 2015; Yu et al., 2016; Martínez-López et al., 2019), open seas (Gómez, 2007), and the polar regions (Ichinomiya et al., 2007; Garzio and Steinberg, 2013; Monti-Birkenmeier et al., 2017; Liang et al., 2018; Li et al., 2022). Aloricate ciliates are grazers of picoplankton and

* Corresponding authors, Li Haibo, E-mail: haiboli@qdio.ac.cn; Zhang Wuchang, ORCID: 0000-0001-7534-8368, E-mail: wuchangzhang@qdio.ac.cn

nanoplankton (Bernard and Rassoulzadegan, 1993) and prey of mesozooplankton (Stoecker and Capuzzo, 1990). Thus, aloricate ciliates are an important linkage between the microbial food web and the traditional food chain, and they play a crucial role in the functioning of marine ecosystems (Stoecker et al., 2017).

Water-column stratification can result in distinct vertical, physical, and chemical properties and create distinct habitats for aloricate ciliates in the marine system (Basu and Mackey, 2018; Loick-Wilde et al., 2019; Romano et al., 2021). Compared with larger and more motile zooplankton, aloricate ciliates have a short life cycle and respond rapidly to environmental changes (Yang et al., 2021). Therefore, aloricate ciliates can form a stable community and quickly adapt to the surrounding seawaters in a stable marine environment, even if the stability only lasts for a short time (Sun et al., 2022).

The upper water column of the Southern Ocean exhibits clear seasonal variation. During spring and summer time, surface water temperature increases, and the melting of sea ice induces water-column stratification (Rozema et al., 2017; Garcia et al., 2020). Global warming affects the polar regions more than other regions on the earth and causes the intense stratification of the Southern Ocean (Sarmiento et al., 2004). The intense stratification will influence the vertical distribution of the plankton community.

The Cosmonaut and Cooperation Seas are located in the Indian sector of the Southern Ocean (East Antarctica). In austral summer, the upper water column of this region is well stratified (Li et al., 2022). Many studies have reported on planktonic ciliates in different environments of the Southern Ocean (Liang et al., 2018; Li et al., 2022). Li et al. (2022) reported on variations in the planktonic ciliate community in different water masses in the Cosmonaut and Cooperation Seas. However, the spatial distribution, especially the vertical variation of the aloricate ciliate community in the stratified Southern Ocean, has never been reported before. In this study, we investigated the aloricate ciliate community at depths of 0 m to 200 m in the Cosmonaut and Cooperation Seas. Our aims were to: (1) determine the vertical variation of aloricate ciliate community in different sampling layers, and (2) describe the abundance and biomass variations of aloricate ciliates in different size classes.

2 Material and methods

Cruise sampling in the Cosmonaut and Cooperation Seas was conducted at 59 stations in 9 transects (Figure 1) onboard the icebreaker R/V *Xuelong 2*, during the 36th Chinese National Antarctic Research Expedition (CHINARE, from November 2019 to January 2020). Water samples were collected using 10-L Niskin bottles on a rosette CTD carousel. One liter of seawater was collected from each sampling point (0, 25, 50, 100, and 200 m at each station). The samples were fixed with Lugol's solution (1% final concentration) in a plastic bottle and kept in a cool and dark place until the time of analysis. A total of 291 samples were collected. Data on temperature, salinity, and chlorophyll-*a* concentration (Chl *a*) were provided by the National Arctic and Antarctic Data Center (http://www.chinare.org.cn).

In the laboratory, the supernatant of each water sample was gently siphoned out after being allowed to settle for at

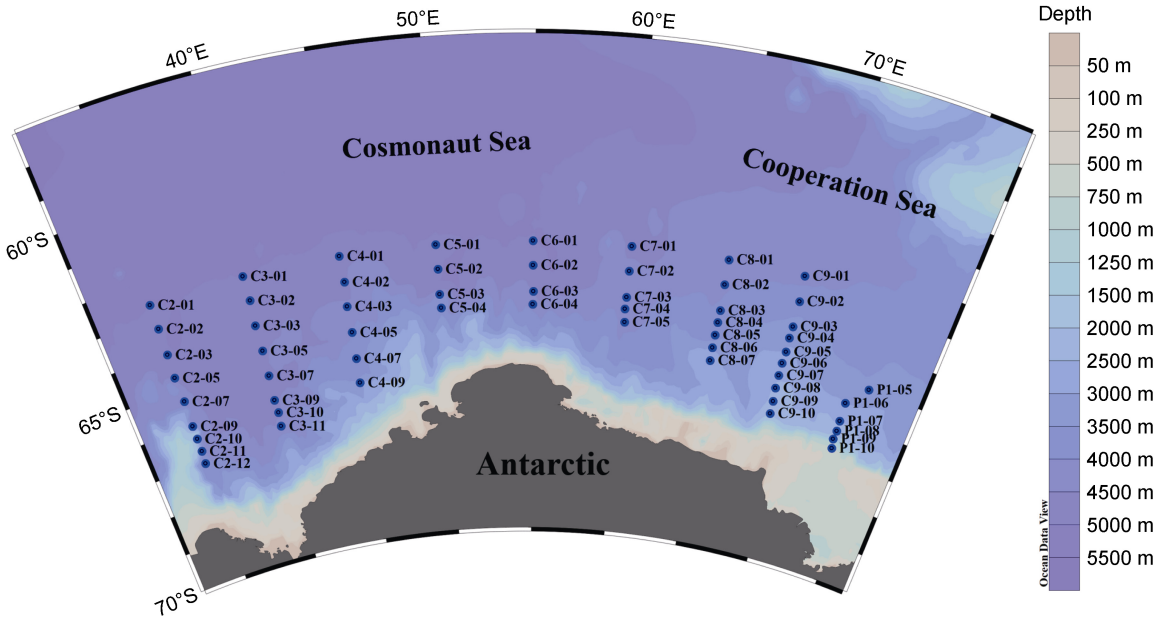

Figure 1 Locations of sampling stations in the Cosmonaut and Cooperation Seas.

least 48 h. This process was repeated until each sample was concentrated to the final volume of 25 mL. Then, concentrated samples were sedimented in Utermöhl counting chambers for at least 24 h, and aloricate ciliates were subsequently counted using an inverted microscope (Olympus IX 71, 100×, or 400×). If the high abundance of aloricate ciliates were found in the previous count, only a part of microscopy fields were counted, while aloricate ciliates with low abundances were counted completely to guarantee accuracy. The length and width of the aloricate ciliates were measured for at least (if possible) 20 individuals. The biovolume of each taxon was estimated from appropriate geometric shapes (e.g., cone, ball, and cylinder). The conversion factor of carbon biomass for aloricate ciliates used in this study was 0.19 pg C·μm^{-3} (Putt and Stoecker, 1989). Aloricate ciliates were not classified into taxa, but into different size classes based on the equivalent spherical diameters. Aloricate ciliates were categorized into 10 size classes, with intervals of 10 μm (i.e., <20 μm, 20–30 μm, 30–40 μm, …, >100 μm). Univariate Spearman correlation analyses were carried out using the statistical program SPSS v16.0 (SPSS Inc., Chicago, IL, USA).

3 Results

3.1 Hydrography

Temperature and salinity were in the ranges of −1.84–1.91°C and 33.27–34.69, respectively. Horizontally, the temperature decreased southward at each transect in each depth except for the 50-m depth, where the temperature was extremely low and relatively homogeneous. The temperature was lower in the middle region than in the eastern and western regions in the surface and 25-m layers, but higher in the 50-m, 100-m, and 200-m layers. The temperature was relatively low from 0 m to 200 m at several of the southeasternmost stations (Figure 2). The distribution pattern of salinity was opposite to that of temperature in the upper 50 m, but similar to the temperature distribution pattern at 100 m and 200 m (Figure 2). Chl *a* was in the range of 0–2.4 μg·L^{-1}. In the upper 50 m, Chl *a* was high in the middle and northern stations of each transect. High values of Chl *a* appeared in the offshore regions of Transects C4 and C9.

Vertically, stratification in the water column was strong in the research area. Temperature and salinity exhibited obvious vertical gradients. Water temperature was lowest in the 50-m layer and increased both upward and downward. Meanwhile, salinity increased from the surface to 200 m at all stations. Chl *a* was high in the upper 50 m and decreased sharply from 50 m to 200 m (Figure 2).

3.2 Aloricate ciliate abundance and biomass

The ranges of aloricate ciliate abundance and biomass were 5–3097 ind·L^{-1} and 0.01–11.40 μg C·L^{-1}, respectively (Table 1). The highest abundance and biomass occurred in the 25-m depth of Station P1-07 and at 0 m of Station C9-01, respectively. Meanwhile, the lowest values of abundance and biomass occurred in 200 m of Station C9-10 and 0 m of Station C9-10, respectively (Figure 3, Table 1).

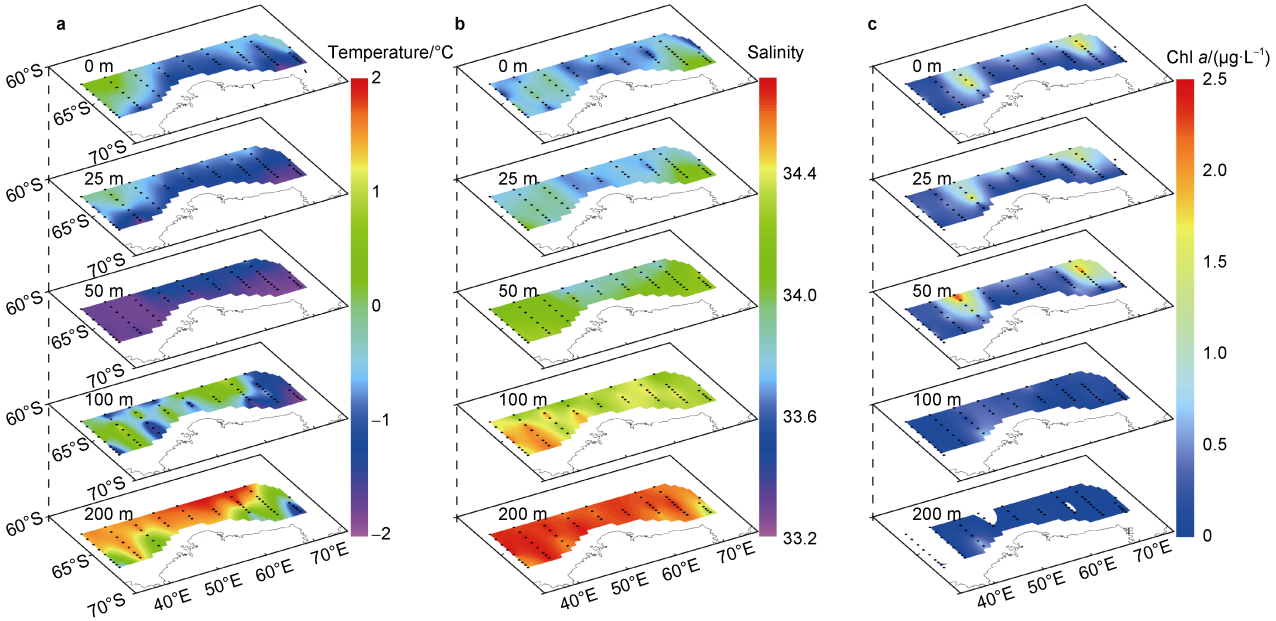

Figure 2 Spatial distribution of temperature (**a**), salinity (**b**), and chlorophyll-*a* concentration (Chl *a*) (**c**) at each sampling layer.

Table 1 Range of abundance and biomass, and occurrence frequency of aloricate ciliates at each sampling layer

Size-class/ μm	0 m (*n*=59)			25 m (*n*=58)			50 m (*n*=59)			100 m (*n*=58)			200 m (*n*=57)			All depths (*n*=291)		
	AR/ (ind·L^{-1})	BR/(μg C·L^{-1})	OF/%	AR/ (ind·L^{-1})	BR/ (μg C·L^{-1})	OF/%	AR/ (ind·L^{-1})	BR/ (μg C·L^{-1})	OF/%	AR/ (ind·L^{-1})	BR/ (μg C·L^{-1})	OF/%	AR/ (ind·L^{-1})	BR/ (μg C·L^{-1})	OF/%	AR/ (ind·L^{-1})	BR/ (μg C·L^{-1})	OF/%
<20	0–523	0–0.18	98.31	0–1768	0–0.59	98.28	8–853	0–0.29	100	0–652	0–0.22	98.28	1–276	0–0.09	100	0–1768	0–0.59	98.97
20–30	5–1175	0.01–4.41	100	3–1790	0–2.79	100	2–764	0–1.19	100	4–523	0.01–0.81	100	1–76	0–0.12	100	1–1790	0–4.41	100
30–40	0–994	0–4.24	98.31	3–397	0.01–1.69	100	3–587	0.01–2.50	100	1–241	0–1.03	100	0–22	0–0.09	87.72	0–994	0–4.24	97.25
40–50	0–243	0–2.20	89.83	0–273	0–2.47	96.55	0–176	0–1.63	96.61	0–152	0–1.38	93.10	0–16	0–0.15	64.91	0–273	0–2.47	88.32
50–60	0–176	0–2.68	76.27	0–162	0–2.68	93.10	0–176	0–2.91	84.75	0–56	0–0.93	79.31	0–4	0–0.07	22.81	0–176	0–2.91	71.48
60–70	0–58	0–1.85	44.07	0–76	0–2.44	50	0–96	0–2.62	55.93	0–24	0–0.66	13.79	0–4	0–0.11	3.51	0–96	0–2.62	33.68
70–80	0–16	0–0.67	8.47	0–22	0–1.07	25.86	0–40	0–1.90	20.34	-	-	0	-	-	0	0–40	0–1.90	11.00
80–90	0–27	0–1.79	15.25	0–44	0–2.91	13.79	0–54	0–3.70	18.64	-	-	0	-	-	0	0–54	0–3.70	9.62
90–100	0–22	0–2.02	3.39	0–22	0–2.01	6.90	0–112	0–8.66	10.17	-	-	0	-	-	0	0–99	0–8.66	4.12
>100	0–3	0–0.54	3.39	0–3	0–0.35	3.45	0–9	0–1.44	3.39	0–3	0–0.58	1.72	-	-	0	0–9	0–1.44	2.41
Total	8–2139	0.01–10.88	100	48–3097	0.39–6.98	100	76–1806	0.18–11.40	100	51–1459	0.07–4.40	100	5–334	0.01–0.45	100	5–3097	0.01–11.40	100

Notes: AR=abundance; BR=biomass; OF=occurrence frequency

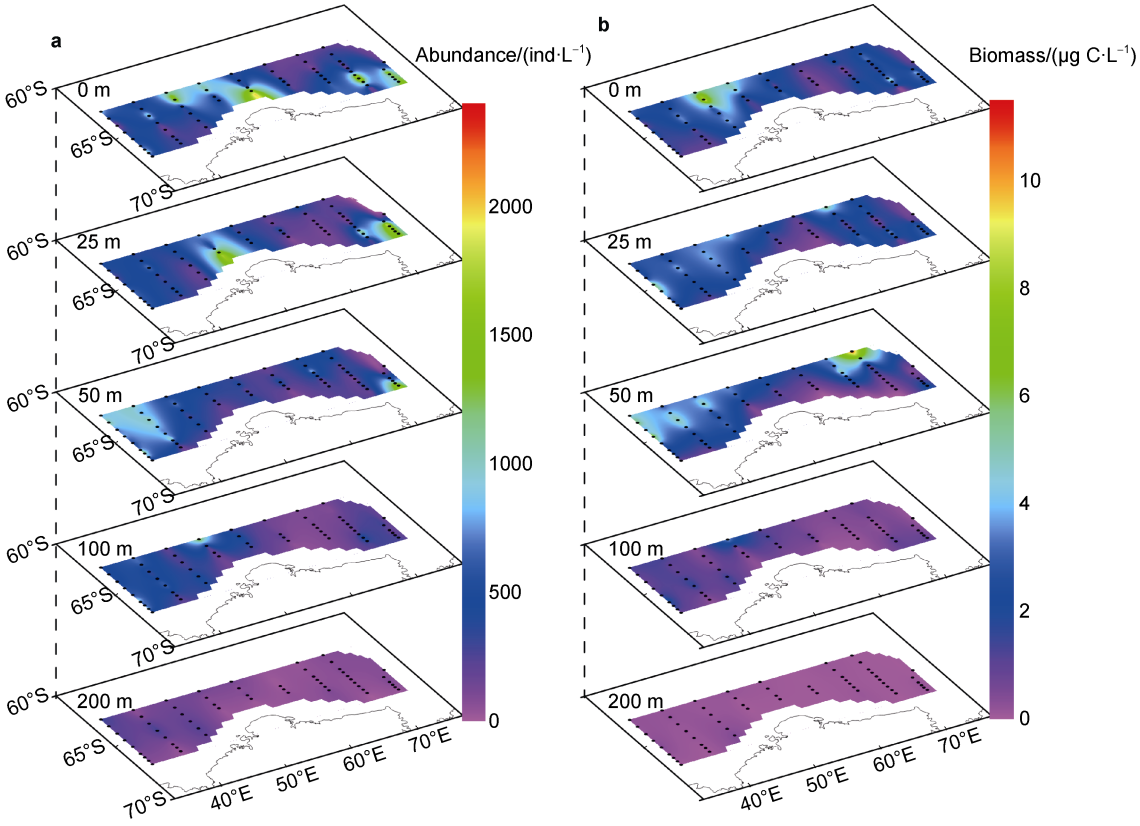

Figure 3 Spatial distribution of aloricate ciliate abundance (**a**) and biomass (**b**) at each sampling layer.

Aloricate ciliates measuring 20–30 μm were the first contributor to total abundance, comprising 38.45% of the total abundance, followed by those measuring <20 μm (28.99%), 30–40 μm (16.78%), and 40–50 μm (8.35%). Aloricate ciliates in the 50–60-μm range only occupied 5.29% of total abundance. However, the biomass structure was clearly different from that of abundance: 50–60-μm aloricate ciliates were the main contributor (21.85%) to total biomass, followed by those measuring 40–50 μm (18.97%), 30–40 μm (17.98%), and 20–30 μm (16.27%). Aloricate ciliates measuring <20 μm had a high abundance proportion, but extremely low biomass proportion (2.47%) (Table 2).

Table 2 Abundance proportion and biomass proportion of different size-class aloricate ciliates at each depth

Size-class	0 m		25 m		50 m		100 m		200 m		All depths	
	AP	BP	AP	BP	AP	BP	AP	BP	AP	BP	AP	BP
<20 μm	13.04%	1.15%	27.19%	2.07%	27.96%	1.89%	49.28%	6.69%	73.71%	20.99%	28.99%	2.47%
20–30 μm	54.34%	24.62%	35.61%	13.23%	34.43%	10.88%	26.64%	16.76%	16.58%	21.91%	38.45%	16.27%
30–40 μm	17.87%	19.28%	16.99%	15.94%	19.62%	16.94%	13.33%	23.00%	5.74%	20.74%	16.78%	17.98%
40–50 μm	7.94%	18.18%	11.38%	22.71%	7.58%	13.85%	7.01%	25.71%	3.22%	24.83%	8.35%	18.97%
50–60 μm	5.31%	21.89%	6.14%	22.32%	6.59%	22.02%	3.28%	21.76%	0.62%	8.63%	5.29%	21.85%
60–70 μm	1.08%	7.68%	1.84%	11.54%	2.18%	11.95%	0.44%	4.81%	0.12%	2.89%	1.40%	9.76%
70–80 μm	0.09%	0.94%	0.35%	3.53%	0.47%	4.40%	0	0	0	0	0.23%	2.65%
80–90 μm	0.25%	4.09%	0.25%	3.59%	0.55%	7.37%	0	0	0	0	0.27%	4.50%
90–100 μm	0.07%	1.69%	0.23%	4.71%	0.56%	8.99%	0	0	0	0	0.22%	4.63%
>100 μm	0.01%	0.48%	0.01%	0.36%	0.06%	1.71%	0.02%	1.27%	0	0	0.02%	0.90%

Notes: AP=abundance proportion; BP=biomass proportion

Horizontally, the distribution of aloricate ciliate abundance and biomass exhibited different patterns in different layers. In the surface and 25-m layers, aloricate ciliate abundance and biomass were higher at the low-temperature and salinity regions. In the 50-m layer, both abundance and biomass were high in low-temperature regions. In the 100-m and 200-m layers, aloricate ciliate distribution was homogeneous in most regions of the research area (Figure 3).

Vertically, the abundance and biomass distributions of aloricate ciliates were clearly different in different regions of the research area. In Transects C2 and C3, aloricate ciliate abundance and biomass increased from the surface to the 50-m layer, then decreased with depth. In other transects, the highest values of abundance and biomass mainly appeared in 0 m and 25 m, except for the two northernmost stations in Transect C9 (Figure 3). The average abundance of aloricate ciliates was highest in the surface layer. It decreased from the surface to 200 m. However, the average biomass of aloricate ciliates increased from the surface to the 50-m layer, then decreased sharply at 200 m (Figure 4).

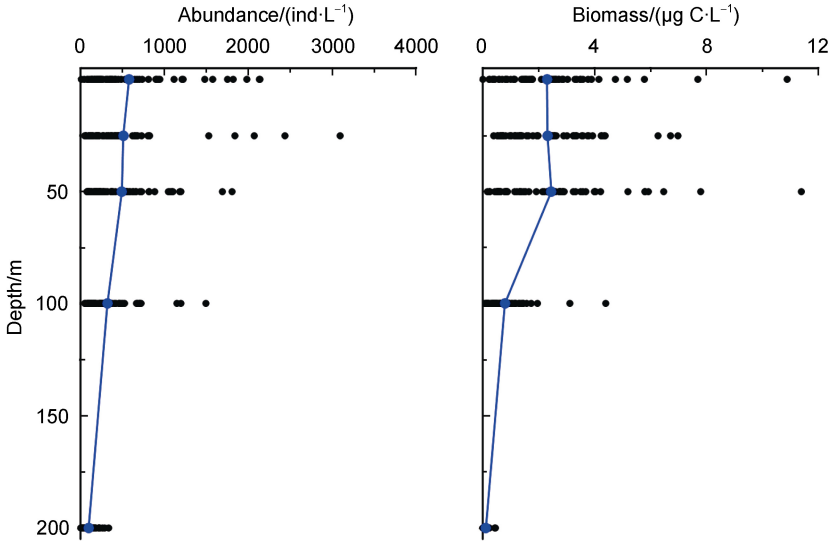

Figure 4 Vertical variation of aloricate ciliate abundance and biomass. The blue dots indicate the average values of each sampling layer, and the blue lines indicate the variation trends of those average values.

Both the abundance and biomass of aloricate ciliates decreased with increasing temperature. The same variation trends were found along the salinity gradient. Aloricate ciliate abundance and biomass increased with the increase in Chl *a* and reached a plateau when Chl *a* was higher than 0.75 μg·L^{-1} (Figure 5).

Correlation analysis showed that aloricate ciliate abundance and biomass exhibited significantly negative correlations with temperature, salinity, and depth, but a significantly positive correlation with Chl *a* (Table 3).

3.3 Vertical variation of aloricate ciliates in different size classes

Aloricate ciliates measuring 20–30 μm were the most common size class. They appeared at all the sampling points, followed by aloricate ciliates measuring <20 μm and 30–40 μm and appeared at 288 and 283 sampling points, respectively. The occurrence frequency of aloricate ciliates larger than 30 μm decreased with the increase in ciliate size (Table 1).

The variation trends of different size class aloricate ciliates along the depth gradient were diverse, but the same vertical trend was seen in the abundance and biomass of aloricate ciliates of the same size class (Figures 5, 6 and 7). The average abundance and biomass of aloricate ciliates measuring <20 μm increased from the surface to the 100-m layer with a very slight fluctuation at 50 m and then decreased until 200 m. Those of the 20–30-μm aloricate ciliates were the highest at the surface and decreased with depth. The vertical variation trend of aloricate ciliates measuring 30–40 μm was similar to those measuring 20–30 μm, but increased slightly at 50 m. Aloricate ciliates ranging from 40 μm to 70 μm had similar vertical distribution patterns. The highest values of aloricate ciliates sized 40–50 μm appeared in 25 m, while those of aloricate ciliates sized 50–60 μm and 60–70 μm appeared in 50 m (Figures 5, 6 and 7). The average abundance and biomass of <20-μm aloricate ciliates in 200 m were similar with those at the surface, while the values of other size classes of aloricate ciliates in 200 m were far less than those in the surface (Figures 5, 6, and 7). Aloricate ciliates in the 70–80-, 80–90-, and 90–100-μm size classes were restricted in the upper 50 m and disappeared in layers deeper than 50 m. Aloricate ciliates in the >100-μm size class occasionally appeared at 0, 25, 50, and 100 m and disappeared at 200 m (Figures 5, 6 and 7; Table 1).

Correlation analysis revealed that the abundance and biomass of aloricate ciliates in most size classes had

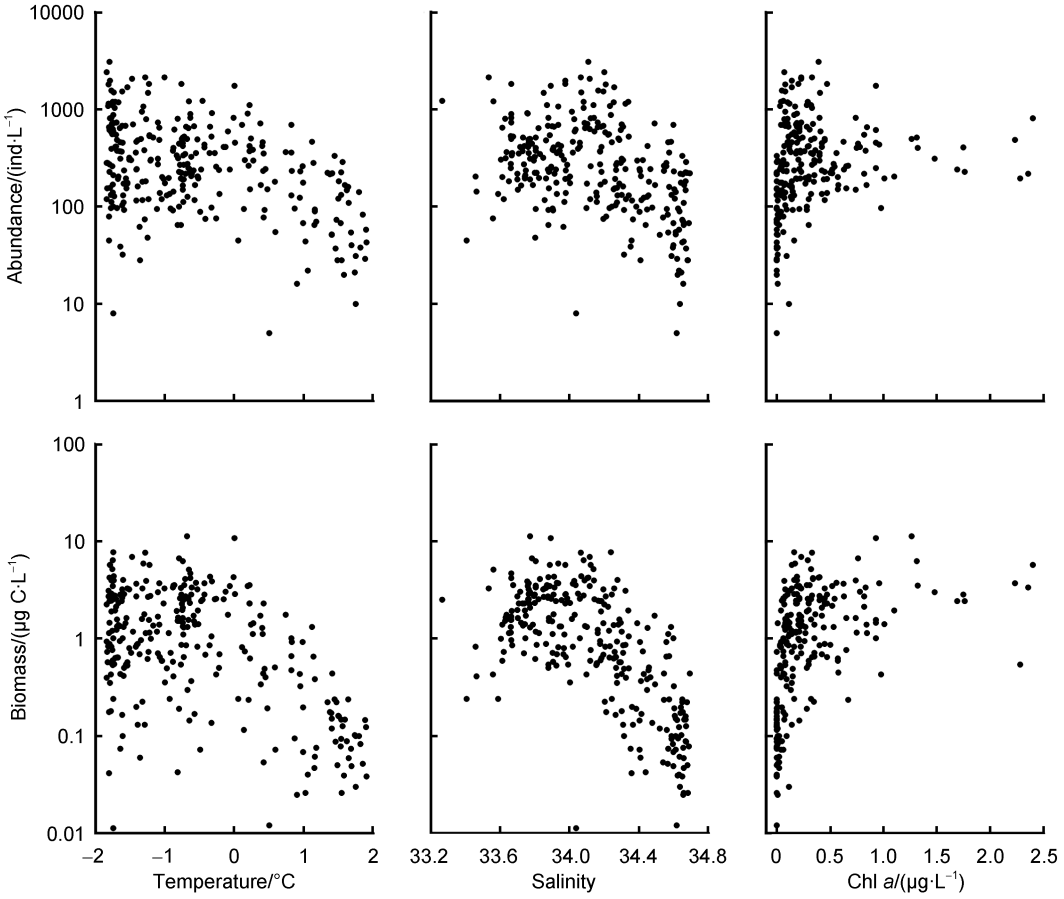

Figure 5 Variation of aloricate ciliate abundance and biomass along the temperature, salinity, and chlorophyll-*a* concentration (Chl *a*) gradient.

significantly negative correlations with temperature, salinity, and depth, and a significantly positive correlation with Chl *a*. Aloricate ciliates in the <20-μm size class exhibited unique relationships with environmental factors. Their abundance and biomass were negatively correlated with temperature and significantly positively correlated with salinity and depth, but there was no significant correlation with Chl *a* (Table 3).

Table 3 Spearman's rank correlation coefficient between environmental factors and aloricate ciliate abundance and biomass

Size-class	Abundance/(ind·L^{-1})				Biomass/(μg C·L^{-1})			
	T/°C	*S*	Chl *a*/(μg·L^{-1})	*D*/m	*T*/°C	*S*	Chl *a*/(μg·L^{-1})	*D*/m
< 20 μm	−0.133*	0.280**	−0.106	0.169**	−0.124*	0.262**	−0.085	0.148*
20–30 μm	−0.467**	−0.465**	0.292**	−0.525**	−0.466**	−0.478**	0.292**	−0.540**
30–40 μm	−0.336**	−0.442**	0.432**	−0.442**	−0.336**	−0.441**	0.431**	−0.441**
40–50 μm	−0.216**	−0.548**	0.570**	−0.492**	−0.216**	−0.548**	0.570**	−0.492**
50–60 μm	−0.247**	−0.507**	0.572**	−0.464**	−0.247**	−0.508**	0.575**	−0.464**
60–70 μm	−0.149*	−0.382**	0.468**	−0.344**	−0.148*	−0.382**	0.467**	−0.345**
70–80 μm	−0.116	−0.214**	0.279**	−0.187**	−0.114	−0.215**	0.279**	−0.188**
80–90 μm	−0.159**	−0.182**	0.234**	−0.210**	−0.160**	−0.181**	0.235**	−0.210**
90–100 μm	−0.078	−0.122*	0.207**	−0.096	−0.078	−0.122*	0.206**	−0.096
> 100 μm	−0.058	−0.056	0.023	−0.077	−0.058	−0.056	0.022	−0.077
Total	−0.359**	−0.410**	0.357**	−0.470**	−0.389**	−0.650**	0.625**	−0.658**

Notes: *T*=temperature; *S*=salinity; Chl *a*=chlorophyll-*a* concentration; *D*=depth; *= Correlation is significant at the 0.05 level (2–tailed); **= Correlation is significant at the 0.01 level (2–tailed)

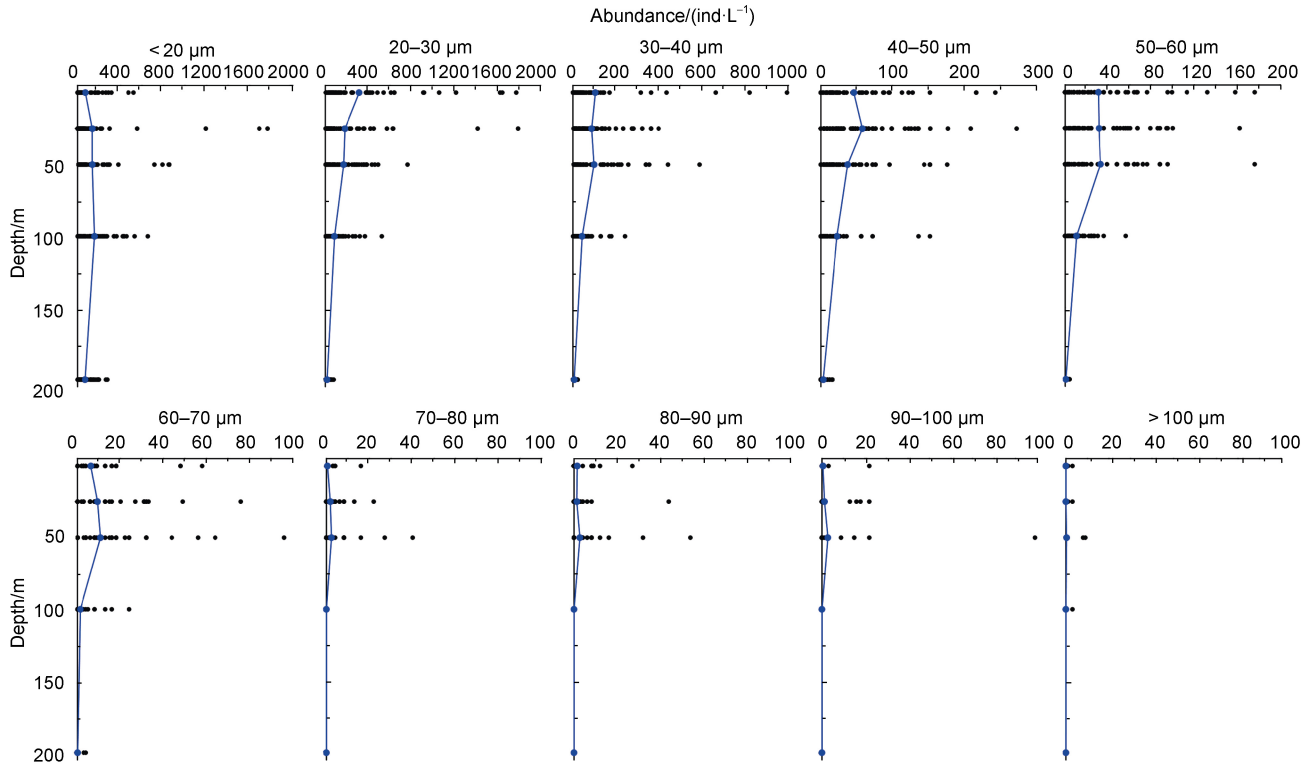

Figure 6 Vertical variation of different size-class aloricate ciliate abundance. The blue dots indicate the average values of each sampling layer, and the lines indicate the variation trends of those average values.

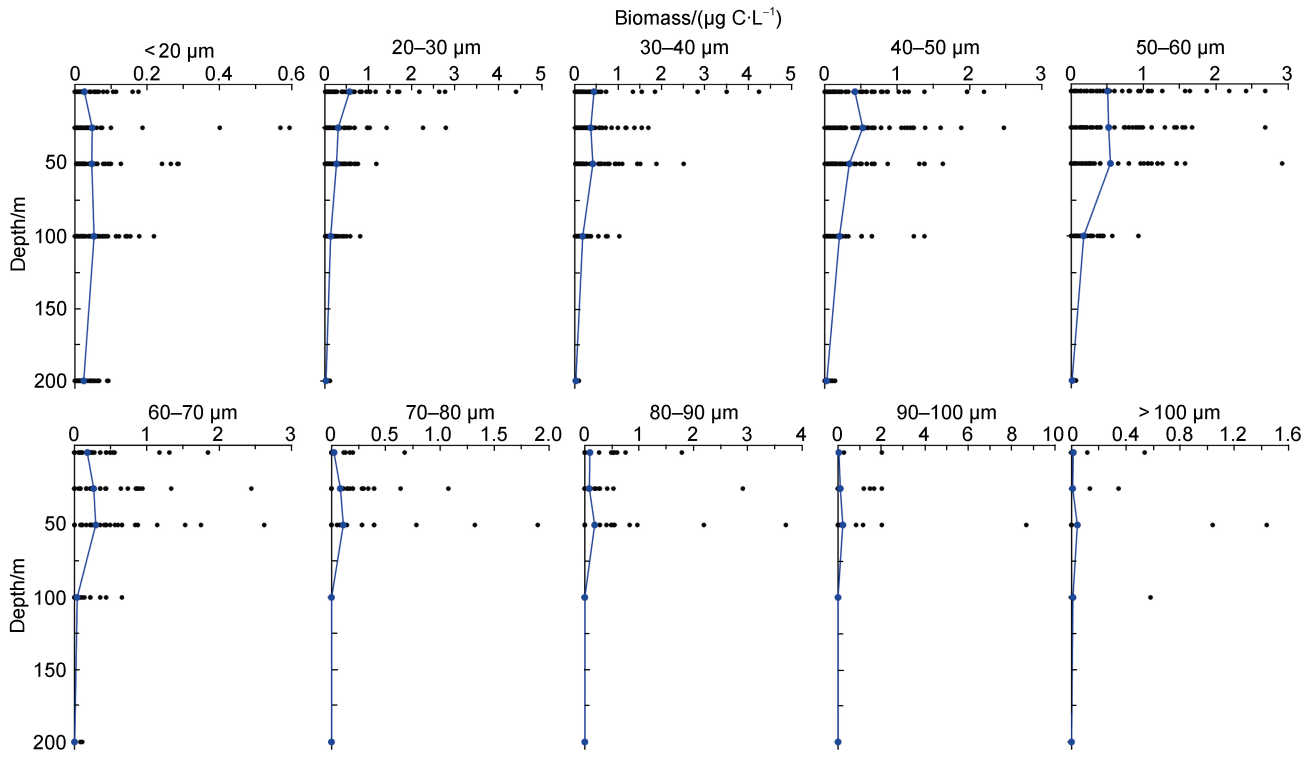

Figure 7 Vertical variation of different size-class aloricate ciliate biomass. The blue dots indicate the average values of each sampling layer, and the lines indicate the variation trends of those average values.

3.4 Structure variation of aloricate ciliate community in different layers

The abundance proportion of aloricate ciliates measuring <20 μm increased from the surface to 200 m. This was the most dominant size class at 100 m (49.28%) and 200 m (73.71%). Aloricate ciliates measuring 20–30 μm were dominant at the surface and in the 25-m layer, and their abundance proportion decreased from 54.34% at 0 m to 16.58% at 200 m. The abundance proportion of 30–40-μm aloricate ciliates was highest at 50 m (19.62%), followed by 0 m (17.87%), and the lowest value appeared at 200 m (5.74%). The variations in the vertical abundance proportions of aloricate ciliates measuring 40–70 μm were the same, increasing at first, then decreasing down to 200 m. However, the highest abundance proportion of aloricate ciliates sized 40–50 μm appeared at 25 m, while those of the other size class appeared at 50 m. The abundance proportion of aloricate ciliates measuring >70 μm were lower than 0.56% in all layers (Figure 8, Table 2).

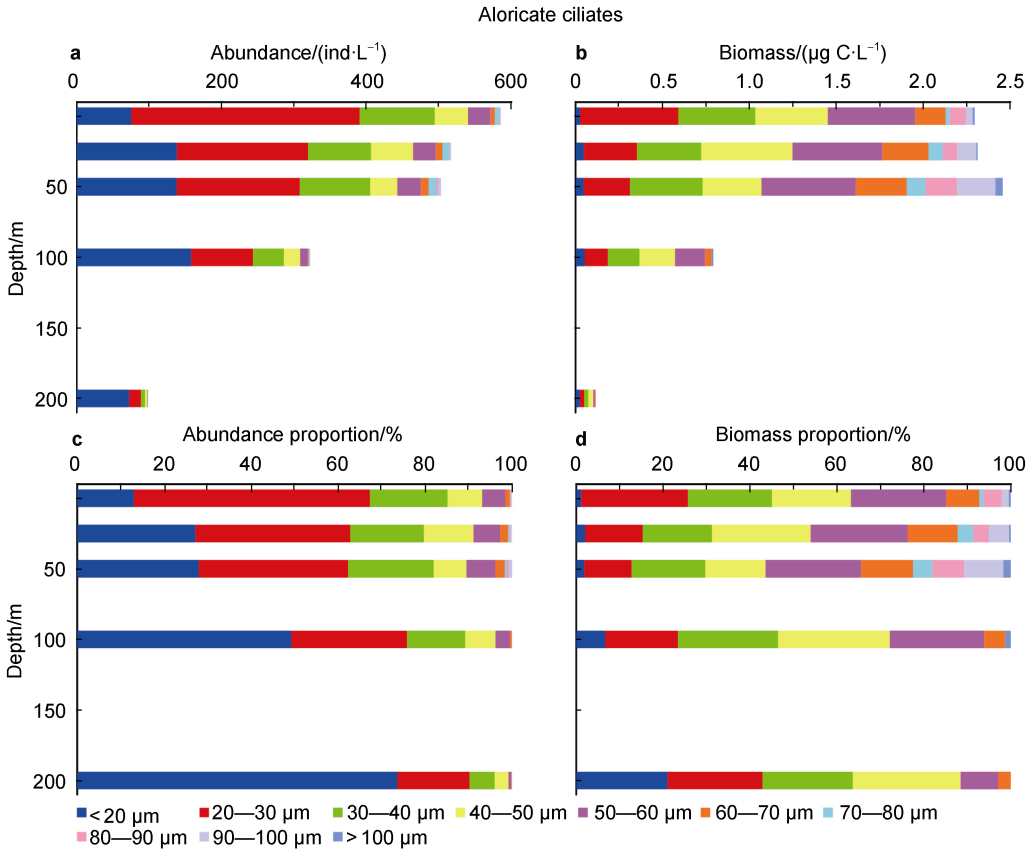

Figure 8 Average abundance (**a**), biomass (**b**), and proportion (**c**, **d**) of each size class of aloricate ciliates at each sampling layer.

Although aloricate ciliates <20 μm had relatively higher abundance proportions in each layer, their biomass proportions were lower than 2.08% from the surface to 50 m and increased to 6.69% at 100 m and to 20.99% at 200 m. The biomass proportion of aloricate ciliates sized 20–30 μm decreased from the surface to 50 m and then increased down to 200 m. The biomass proportion of 30–40-μm aloricate ciliates was the lowest at 25 m (15.94%) and highest at 100 m (23.00%). The biomass proportions of aloricate ciliates measuring 40–50 μm were higher at 100 m and 200 m. With increased depth, the biomass proportions of aloricate ciliates measuring 50–60 μm and 60–70 μm increased at first and then decreased, with the highest values at 25 m and 50 m, respectively (Figure 8).

4 Discussion

4.1 Aloricate ciliate abundance and biomass

Many studies have reported large ranges of aloricate ciliate abundance in the Southern Ocean. Aloricate ciliate abundance was in the range of 387–695 ind·L^{-1} in the Atlantic sector (south of 60°S) of the Southern Ocean (Froneman and Perissinotto, 1996), 80–39969 ind·L^{-1} in the Western Antarctic Peninsula (Garzio and Steinberg, 2013), 10–1900 ind·L^{-1} in the Scotia Sea (Sushin et al., 1986; Garrison et al., 1993), 0–9000 ind·L^{-1} in the Weddell Sea (Buck and Garrison, 1983; Garrison and Buck, 1989; Monti-Birkenmeier et al., 2017), 1262–2330 ind·L^{-1} in the

Ross Sea (Safi et al., 2012), and 1–2770 ind·L^{-1} in the Prydz Bay (Liang et al., 2018). In our study, aloricate ciliate abundance (5–3097 ind·L^{-1}) was in the lower end of previous data.

Aloricate ciliates measuring <20 μm were the main contributor to total abundance in neritic waters (Lynn et al., 1991), the equatorial Pacific Ocean (Yang et al., 2004), and the Southern Ocean (Liang et al., 2018). Yang et al. (2004) found that the abundance of <20-μm aloricate ciliates accounted for 49.9% of the total abundance in the northeast equatorial Pacific Ocean. Liang et al. (2018) reported that <20-μm aloricate ciliates represented approximately 40% of total abundance in the Prydz Bay. In our study, <20-μm aloricate ciliates only contributed 28.99% to the total abundance, and this value was less than those in previous studies. Although <20-μm aloricate ciliates contributed a large part to total abundance, it only accounted for a small portion of aloricate ciliates biomass (Yang et al., 2004; Christaki et al., 2008). Our results were consistent with the following: the <20-μm aloricate ciliate biomass proportion was <10% from the surface to 100 m and approximately 20% at 200 m.

Aloricate ciliates <30 μm contributed to 75.5%, 54.6%, and 56.7% of aloricate ciliate abundance in the tropical West Pacific, the Bering Sea, and the Arctic Ocean, respectively (Wang et al., 2020). Our results indicate that <20-μm and 20–30-μm aloricate ciliates made up 67.44% of the total abundance; this value was lower than that of the tropical West Pacific but higher than those of the Bering Sea and the Arctic Ocean.

In stratified Arctic and sub-Arctic waters, mixotrophic ciliates usually dominate the ciliate community (Putt, 1990; Suzuki and Taniguchi, 1998; Levinsen et al., 2000). Meanwhile, <30-μm mixotrophic ciliates were the main contributor to total ciliate abundance (Romano et al., 2021). In the present study, the water column was well stratified, which was beneficial to the development of small mixotrophic ciliates (Romano et al., 2021). Therefore, we speculate that the <20-μm and 20–30-μm aloricate ciliates in our study are mainly composed of mixotrophic ciliates.

4.2 Vertical variation of aloricate ciliate community structure

Several studies have reported on the vertical distribution of the aloricate ciliate community structure in different marine environments (Wang et al., 2020, 2021, 2022). The abundance variation trends differ extremely between those in our study and those in tropical waters. In our study, aloricate ciliate abundance decreased from the surface to the 200-m layer, while the abundance showed bimodal patterns (i.e., the peaks occurred in the surface and the deep chlorophyll maximum (DCM) layers) along the vertical profiles in the tropical seamount regions (Wang et al., 2021). In the open tropical Pacific Ocean, the abundance of aloricate ciliates was relatively homogeneous in the upper 100-m depth, with a higher abundance near the surface (Gómez, 2007).

The abundance proportion of <20-μm aloricate ciliates increased from the surface to 200 m in tropical seamount regions (Wang et al., 2021). It first decreased, then increased to the 200-m layer, before reaching the lowest values in the 75-m layer in the tropical Pacific and the Bering Sea and the 50-m layer in the Arctic Ocean (Wang et al., 2020). The vertical variation of the <20-μm aloricate ciliate abundance proportion in our study showed a similar but much sharper trend compared with that in the tropical seamount regions. In the seamount regions, the abundance proportion varied from approximately 40% in the surface water to approximately 55% in the 200-m layer (Wang et al., 2021). In our study, it increased from 12.37% in the surface to 63.25% in the 200-m layer.

The variation trend in the abundance proportion of 20–30-μm aloricate ciliates along the depth gradient in our study was clearly different from that of previous studies. In this study, it decreased from 47.99% in the surface to 22.91% in the 200-m layer with a slight increase in the 50-m layer. In the tropical Pacific Ocean, tropical seamount regions, the Bering Sea, and the Arctic Ocean, the 20–30-μm size-class contribution rate was relatively constant along the depth gradient (Wang et al., 2020, 2021, 2022).

Aloricate ciliates measuring <20 μm contributed to more than 40% of aloricate ciliate abundance and were the most abundant group from the surface to the 200-m depth in the tropical Pacific. However, in the Bering Sea and the Arctic Ocean, aloricate ciliates >30 μm were the dominant component in most layers except for the 200-m layer, where the aloricate ciliates <20 μm contributed to more than 40% aloricate ciliate abundance (Wang et al., 2020). In the tropical seamounts of Yap, Mariana, and Caroline, aloricate ciliates measuring <20 μm comprised more than 30% of aloricate ciliate abundance at each depth (Wang et al., 2021). In the present study, 20–30-μm aloricate ciliates were the most dominant group and <20-μm aloricate ciliates contributed to <30% of the total abundance from the surface to the 50-m layer.

The abundance proportion of aloricate ciliates >30 μm in this study showed similar variation trends along the vertical profiles in the tropical West Pacific, the Bering Sea, and the Arctic Ocean (Wang et al., 2020). In both our study and Wang et al. (2020), the abundance proportion of aloricate ciliates >30 μm increased from the surface to the layers between 30–75 m, and then decreased to the 200-m layer.

Aloricate ciliates measuring >50 μm were more abundant in the upper 85 m than below in the ice-edge zone of the Weddell and Scotia Seas during the austral winter, and they were not found in samples from 190 m and 200 m (Gowing and Garrison et al., 1992). In our study, aloricate ciliates measuring >50 μm were more abundant in the upper 50 m, accounting for more than 10% of total abundance,

and only accounting for <5% and about 1% at 100 m and 200 m, respectively.

4.3 Impact of water-column stratification on the distribution of aloricate ciliates

In this study, the water column was well stratified. Water-column stratification is essential for phytoplankton development and governs phytoplankton succession (Rozema et al., 2017; Garcia et al., 2019). The stratification of the water column favors the development of small eukaryotic algae and thus affects the ciliate community (Garcia et al., 2019; Romano et al., 2021). In the Red Sea, the ciliate community was clearly affected by water-column stratification, as both abundance and biomass declined strongly along the vertical profile during summer stratification, with the highest average values in the surface layer (Claessens et al., 2008). The average abundance decreased along the depth gradient in this study, which was consistent with the results of Claessens et al. (2008). But the highest value of average biomass appeared in the 50-m layer in our study.

During the stratification period in the oligotrophic Eastern Mediterranean, very small (<18 μm) and small (18–30 μm) ciliates were distributed throughout the water column, whereas the species measuring >50 μm were found only above the 50-m layer (Romano et al., 2021). In the seamount regions of the tropical Pacific Ocean, aloricate ciliates measuring >50 μm contributed less than 10% to the total abundance in the 200-m layer (Wang et al., 2020). In the present study, the abundance proportion of aloricate ciliates measuring >50 μm decreased sharply in the 100-m and 200-m layers, which is consistent with the results of Romano et al. (2021) and Wang et al. (2020).

The stratification will hinder the exchange of nutrients between the upper and lower waters (Cermeño et al., 2008), causing oligotrophic conditions in the deep waters of the euphotic layer. The oligotrophic conditions favor the small ciliates that feed on pico-bacterioplankton (Romano et al., 2021). Thus, the importance of small ciliates increases with the depth gradient in the euphotic layer. The aloricate ciliate community structure in our study is a universal phenomenon in the Antarctic and perhaps other stratified waters around the world. In the Southern Ocean, water-column stratification becomes more obvious with increased global warming. The input of fresh and iron-rich melting ice water will enhance vertical stratification (Sarmiento et al., 2004; Kim and Kim, 2021). Thus, we predict that the importance of small aloricate ciliates will increase with ongoing global warming.

5 Conclusion

The aloricate ciliate distribution and community structure were studied in the Cosmonaut and Cooperation Seas of the Southern Ocean. In a well-stratified water column, the aloricate ciliate community structure changed dramatically along the depth gradient, and the smaller aloricate ciliates became more important from the surface to the 200-m layer. We clarified the distribution pattern of the aloricate ciliate community in a well-stratified water column of the Southern Ocean. Our results are important for predicting trends in microzooplankton community variation, along with the intensified stratification of the Southern Ocean.

Acknowledgements This work was supported by the National Polar Special Program "Impact and Response of Antarctic Seas to Climate Change" (Grant no. IRASCC 01-02-01D) and the National Natural Science Foundation of China (Grant nos. 41706192, 41806178). We are thankful to the 36th CHINARE for providing logistical support and environmental data. We thank the crew on the R/V *Xuelong 2* for their support and assistance during sampling. We are deeply grateful to the Associate Editor and two anonymous reviewers for their helpful comments and suggestions, which substantially improved the manuscript.

References

Basu S, Mackey K. 2018. Phytoplankton as key mediators of the biological carbon pump: their responses to a changing climate. Sustainability, 10(3): 869, doi:10.3390/su10030869.

Bernard C, Rassoulzadegan F. 1993. The role of picoplankton (cyanobacteria and plastidic picoflagellates) in the diet of tintinnids. J Plankton Res, 15(4): 361-373, doi:10.1093/plankt/15.4.361.

Buck K R, Garrison D L. 1983. Protists from the ice-edge region of the Weddell Sea. Deep Sea Res A Oceanogr Res Pap, 30(12): 1261-1277, doi:10.1016/0198-0149(83)90084-5.

Cermeño P, Dutkiewicz S, Harris R P, et al. 2008. The role of nutricline depth in regulating the ocean carbon cycle. Proc Natl Acad Sci USA, 105(51): 20344-20349, doi:10.1073/pnas.0811302106.

Christaki U, Obernosterer I, Van Wambeke F, et al. 2008. Microbial food web structure in a naturally iron-fertilized area in the Southern Ocean (Kerguelen Plateau). Deep Sea Res Part II Top Stud Oceanogr, 55(5-7): 706-719, doi:10.1016/j.dsr2.2007.12.009.

Claessens M, Wickham S A, Post A F, et al. 2008. Ciliate community in the oligotrophic Gulf of Aqaba, Red Sea. Aquat Microb Ecol, 53: 181-190, doi:10.3354/ame01243.

Froneman P, Perissinotto R. 1996. Microzooplankton grazing in the Southern Ocean: implications for the carbon cycle. Mar Ecol, 17(1/3): 99-115, doi:10.1111/j.1439-0485.1996.tb00493.x.

Garcia M D, Dutto M S, Chazarreta C J, et al. 2020. Micro- and mesozooplankton successions in an Antarctic coastal environment during a warm year. PLoS One, 15(5): e0232614, doi:10.1371/journal.pone.0232614.

Garcia M D, Severini M D, Spetter C, et al. 2019. Effects of glacier melting on the planktonic communities of two Antarctic coastal areas (Potter Cove and Hope Bay) in summer. Reg Stud Mar Sci, 30: 100731, doi:10.1016/j.rsma.2019.100731.

Garrison D L, Buck K R, Gowing M M. 1993. Winter plankton assemblage in the ice edge zone of the Weddell and Scotia Seas: composition, biomass and spatial distributions. Deep Sea Res Part I Oceanogr Res Pap, 40(2): 311-338, doi:10.1016/0967-0637(93)90006-O.

Garrison D L, Buck K R. 1989. Protozooplankton in the Weddell Sea, Antarctica: abundance and distribution in the ice-edge zone. Polar Biol, 9(6): 341-351, doi:10.1007/BF00442524.

Garzio L M, Steinberg D K. 2013. Microzooplankton community composition along the Western Antarctic Peninsula. Deep Sea Res Part I Oceanogr Res Pap, 77: 36-49, doi:10.1016/j.dsr.2013.03.001.

Gómez F. 2007. Trends on the distribution of ciliates in the open Pacific Ocean. Acta Oecologica, 32(2): 188-202, doi:10.1016/j.actao.2007.04.002.

Gowing M M, Garrison D L. 1992. Abundance and feeding ecology of larger protozooplankton in the ice edge zone of the Weddell and Scotia Seas during the austral winter. Deep Sea Res A Oceanogr Res Pap, 39(5): 893-919, doi:10.1016/0198-0149(92)90128-G.

Ichinomiya M, Honda M, Shimoda H, et al. 2007. Structure of the summer under fast ice microbial community near Syowa Station, eastern Antarctica. Polar Biol, 30(10): 1285-1293, doi:10.1007/s00300-007-0289-8.

Kim S U, Kim K Y. 2021. Impact of climate change on the primary production and related biogeochemical cycles in the coastal and sea ice zone of the Southern Ocean. Sci Total Environ, 751: 141678, doi:10.1016/j.scitotenv.2020.141678.

Levinsen H, Turner J T, Nielsen T G, et al. 2000. On the trophic coupling between protists and copepods in Arctic marine ecosystems. Mar Ecol Prog Ser, 204: 65-77, doi:10.3354/meps204065.

Li H B, Chen X, Denis M, et al. 2020. Seasonal and spatial variation of pelagic microbial food web structure in a semi-enclosed temperate bay. Front Mar Sci, 7: 589566, doi:10.3389/fmars.2020.589566.

Li H B, Xu Z Q, Mou W X, et al. 2022. Planktonic ciliates in different water masses of Cosmonaut and Cooperation Seas (Indian sector of the Southern Ocean) during austral summer. Polar Biol, 45(6): 1059-1076, doi:10.1007/s00300-022-03057-w.

Li H B, Xu Z Q, Zhang W C, et al. 2016. Boreal tintinnid assemblage in the Northwest Pacific and its connection with the Japan Sea in summer 2014. PLoS One, 11(4): e0153379, doi:10.1371/journal.pone.0153379.

Liang C, Li H B, Dong Y, et al. 2018. Planktonic ciliates in different water masses in open waters near Prydz Bay (East Antarctica) during austral summer, with an emphasis on tintinnid assemblages. Polar Biol, 41(11): 2355-2371, doi:10.1007/s00300-018-2375-5.

Loick-Wilde N, Fernández-Urruzola I, Eglite E, et al. 2019. Stratification, nitrogen fixation, and cyanobacterial bloom stage regulate the planktonic food web structure. Glob Chang Biol, 25(3): 794-810, doi:10.1111/gcb.14546.

Lynn D H, Roff J C, Hopcroft R R. 1991. Annual abundance and biomass of aloricate ciliates in tropical neritic waters off Kingston, Jamaica. Mar Biol, 110(3): 437-448, doi:10.1007/BF01344362.

Martínez-López A, Pérez-Morales A, Ayala-Rodríguez G A, et al. 2019. Abundance and seasonal variability of aloricate ciliates and tintinnids in a eutrophic coastal lagoon system of the Gulf of California, Mexico. Reg Stud Mar Sci, 32: 100814, doi:10.1016/j.rsma.2019.100814.

Monti-Birkenmeier M, Diociaiuti T, Umani S F, et al. 2017. Microzooplankton composition in the winter sea ice of the Weddell Sea. Antarct Sci, 29(4): 299-310, doi:10.1017/s0954102016000717.

Putt M. 1990. Abundance, chlorophyll content and photosynthetic rates of ciliates in the Nordic Seas during summer. Deep Sea Res A Oceanogr Res Pap, 37(11): 1713-1731, doi:10.1016/0198-0149(90)90073-5.

Putt M, Stoecker D K. 1989. An experimentally determined carbon: volume ratio for marine "oligotrichous" ciliates from estuarine and coastal waters. Limnol Oceanogr, 34(6): 1097-1103, doi:10.4319/lo.1989.34.6.1097.

Romano F, Symiakaki K, Pitta P. 2021. Temporal variability of planktonic ciliates in a coastal oligotrophic environment: mixotrophy, size classes and vertical distribution. Front Mar Sci, 8: 641589, doi:10.3389/fmars.2021.641589.

Rozema P D, Biggs T, Sprong P A A, et al. 2017. Summer microbial community composition governed by upper-ocean stratification and nutrient availability in northern Marguerite Bay, Antarctica. Deep Sea Res Part II Top Stud Oceanogr, 139: 151-166, doi:10.1016/j.dsr2.2016.11.016.

Safi K A, Robinson K V, Hall J A, et al. 2012. Ross Sea deep-ocean and epipelagic microzooplankton during the summer-autumn transition period. Aquat Microb Ecol, 67(2): 123-137, doi:10.3354/ame01588.

Sarmiento J L, Gruber N, Brzezinski M A, et al. 2004. High-latitude controls of thermocline nutrients and low latitude biological productivity. Nature, 427(6969): 56-60, doi:10.1038/nature02127.

Stoecker D K, Capuzzo J M. 1990. Predation on protozoa: its importance to zooplankton. J Plankton Res, 12(5): 891-908, doi:10.1093/plankt/12.5.891.

Stoecker D K, Hansen P J, Caron D A, et al. 2017. Mixotrophy in the marine plankton. Ann Rev Mar Sci, 9: 311-335, doi:10.1146/annurev-marine-010816-060617.

Sun P, Liao Y Y, Wang Y, et al. 2022. Contrasting community composition and co-occurrence relationships of the active pico-sized haptophytes in the surface and subsurface chlorophyll maximum layers of the Arctic Ocean in summer. Microorganisms, 10(2): 248, doi:10.3390/microorganisms10020248.

Sushin V A, Samyshev E Z, Gaydamak A I. 1986. The significance of infusoria in Antarctic plankton communities. Oceanology, 26(6): 982-988.

Suzuki T, Taniguchi A. 1998. Standing crops and vertical distribution of four groups of marine planktonic ciliates in relation to phytoplankton chlorophyll *a*. Mar Biol, 132(3): 375-382, doi:10.1007/s00227005 0404.

Wang C F, Li H B, Dong Y, et al. 2021. Planktonic ciliate trait structure variation over Yap, Mariana, and Caroline seamounts in the tropical western Pacific Ocean. J Ocean Limnol, 39(5): 1705-1717, doi:10.1007/s00343-021-0476-4.

Wang C F, Li H B, Xu Z Q, et al. 2020. Difference of planktonic ciliate communities of the tropical West Pacific, the Bering Sea and the Arctic Ocean. Acta Oceanol Sin, 39(4): 9-17, doi:10.1007/s13131-020-1541-0.

Wang C F, Yang M Y, He Y, et al. 2022. Hydrographic feature variation caused pronounced differences in planktonic ciliate community in the Pacific Arctic region in the summer of 2016 and 2019. Front Microbiol, 13: 881048, doi:10.3389/fmicb.2022.881048.

Yang E J, Choi J K, Hyun J H. 2004. Distribution and structure of heterotrophic protist communities in the northeast equatorial Pacific Ocean. Mar Biol, 146(1): 1-15, doi:10.1007/s00227-004-1412-9.

Yang E J, Jiang Y, Lee S H. 2016. Microzooplankton herbivory and community structure in the Amundsen Sea, Antarctica. Deep Sea Res Part II Top Stud Oceanogr, 123: 58-68, doi:10.1016/j.dsr2.2015.06.001.

Yang J P, Chen Z J, Chen D X, et al. 2021. Spatial distribution of the

microzooplankton communities in the northern South China Sea: insights into their function in microbial food webs. Mar Pollut Bull, 162: 111898, doi:10.1016/j.marpolbul.2020.111898.

Yu Y, Zhang W C, Feng M P, et al. 2016. Differences in the vertical distribution and response to freshwater discharge between aloricate ciliates and tintinnids in the East China Sea. J Mar Syst, 154: 103-109, doi:10.1016/j.jmarsys.2015.02.005.

Zhang C X, Zhang W C, Ni X B, et al. 2015. Influence of different water masses on planktonic ciliate distribution on the East China Sea shelf. J Mar Syst, 141: 98-111, doi:10.1016/j.jmarsys.2014.09.003.